Hindawi
Advances in Civil Engineering
Volume 2020, Article ID 3239793, 14 pages
https://doi.org/10.1155/2020/3239793

Research Article

Synergetic Effect of Nano-ZnO and Trinidad Lake Asphalt for Antiaging Properties of SBS-Modified Asphalt

Yiqun Zhan, Jun Xie, Yulin Wu, and Yifan Wang

School of Traffic and Transportation Engineering, Changsha University of Science & Technology, Changsha 410114, China

Correspondence should be addressed to Jun Xie; howardxj@csust.edu.cn

Received 13 August 2019; Revised 15 January 2020; Accepted 5 February 2020; Published 26 February 2020

Academic Editor: Emanuele Brunesi

In order to address the influence of aging on the performance degradation of SBS-modified asphalt, a composite modification of SBS-modified asphalt by nano-zinc oxide (nano-ZnO) and Trinidad Lake asphalt (TLA) was proposed. Several tests were conducted after adding nano-ZnO and TLA to SBS-modified asphalt, including a rotary film oven test (RTFOT), ultraviolet aging (UV), and the pressure aging vessel test (PAV). The conventional physical index, rheological index, and four-component content of SBS-modified asphalt before and after three aging modes were tested, and the characteristic functional groups in SBS-modified asphalt were tracked and analyzed by Fourier transform infrared spectroscopy (FTIR). The results show that the effects of aging on the rheological properties of SBS-modified asphalt are clearly reduced by adding different proportions of nano-ZnO and TLA in the process of thermal oxygen aging and the ultraviolet aging test, and the antiaging ability of SBS-modified asphalt is clearly improved. To improve the conventional performance and rheological properties of SBS-modified asphalt, an incorporation ratio of 3% nano-ZnO + 25% TLA was proposed. At the same time, the increased rate of heavy components and the change index of the colloidal instability index in the SBS-modified asphalt under the blending ratio were significantly lower than the blank SBS-modified asphalt samples in the same aging mode. FTIR spectra also showed that SBS-modified asphalt performance deterioration were mainly caused by long-term aging and ultraviolet aging. The addition of nano-ZnO and TLA effectively reduced the increase of carbonyl groups and the breakage of the C=C double bond in butadiene and synergistically improved the comprehensive aging resistance of SBS-modified asphalt. Therefore, the use of this modification is an effective method to solve the aging problem of SBS-modified asphalt.

1. Introduction

Styrene-butadiene-styrene copolymer- (SBS) modified asphalt had been widely used in the pavement industry due to its excellent high temperature performance and low temperature sensitivity [1]. However, SBS-modified asphalt still has serious aging problems, which eventually causes asphalt concrete to lose its function prematurely and affects the service life of asphalt pavement [1–4]. Therefore, the aging of SBS-modified asphalt is an urgent problem that requires further research.

With the development of nano-materials technologies, more and more nano-materials have been used in asphalt modifications. Zhang et al. [5] added a variety of inorganic nanoparticles ($CaCO_3$, ZnO, TiO_2, and Fe_3O_4) to the asphalt and studied its high and low temperature and aging properties. As a result, it was found that nano-ZnO showed the best antiaging performance and high-temperature performance among various particles. Sun et al. [6] found that the ductility of nano-TiO_2 modified asphalt was relatively stable, and the softening point increase after UV aging was small, which shows that nano-TiO_2 particles effectively improved the anti-ultraviolet-oxidation ability of asphalt. Saltan et al. [7] prepared nano-SiO_2 asphalt and its mixture. The research found that the basic properties of asphalt have been improved. After short-term and long-term aging, nano-silica modified asphalt mixture still had good rutting resistance and fatigue performance. Sun et al. [8] added different nanoparticles to the polymer modified asphalt, and the research results found that the modified asphalt mixture containing 0.5% SiO_2 + 5% SBR + 1% PE had the best high- and low-temperature performance. The short-term aging performance was also significantly improved, and good results have been achieved in actual engineering. Liu et al. [9] used different surface

modifiers to modify the surface of nano-ZnO. It was found that nano-ZnO-modified asphalt showed the smallest VAI value and carbonyl index after UV aging, indicating that it had good resistance to ultraviolet aging. The team of Yao et al. [10, 11] used infrared spectroscopy to study the change of internal functional groups after aging of various nano-clay and silica-modified asphalt. The aging process of asphalt was analyzed and summarized. Finally, it was determined that nano-materials can better improve the antiaging ability of asphalt. Du et al. [12] found that the addition of nano-zinc oxide helped the formation of honeycomb structure in asphalt, and it leads to the separation of asphaltenes from the matrix. Under the same UV aging, the viscosity of nano-zinc oxide modified asphalt increased more slowly and can significantly reduce the carbonyl index of asphalt. Arabani et al. [13] conducted laboratory experiments to study the effect of nano-ZnO on improving the mechanical properties of hot-mixed asphalt (HMA). The results show that nano-ZnO particles can reduce the permanent deformation of HMA pavement. Xiao and Li [14] found that the high-temperature or low-temperature properties and short-term heat-resistant oxidative aging properties of styrene-butadiene-styrene copolymer (SBS) modified asphalt can be improved by adding nano-ZnO. Chen et al. [15] prepared nano-zinc oxide modified asphalt by a high-speed shear method and found that when the content reached 4%, the matrix asphalt mixture had the best high-temperature stability, water stability, and low-temperature crack resistance. Sun et al. [16] found that nano-zinc oxide can significantly improve the performance of asphalt mixtures. The performance of nanocomposite modified asphalt is better than polymer modified asphalt to a certain extent. At the same time, nano-zinc oxide can make the effect of SBS-modifier more obvious. Su et al. [17] found that adding certain amounts of ZnO, TiO_2, and SBS modifiers to the matrix asphalt can greatly improve the antiaging performance of the asphalt mixture. At the same time, they recommended the use of an AC-20 asphalt mixture prepared by composite modified asphalt as the surfacing material to resist the damage caused by extreme high-temperature weather. In many studies, the effect of improving the antiaging ability of asphalt with nano-ZnO was more obvious.

As mentioned, nano-materials had been widely used in asphalt modification for their ability to improve the photo-oxidation performance of asphalt materials [18, 19]; however, they have limited influence on the antioxidation aging ability of asphalt and had some limitations in use. Li et al. [20] studied the aging of TLA and found that the viscosity aging index (VAI) and softening point increment (SPI) of a thin film oven test (TFOT) and pressure aging vessel (PAV) test were significantly lower than those of ordinary asphalt and suggested that TLA could enhance the antioxidant aging ability of asphalt. Liu et al. [21] studied the effect of different doses of TLA on the aging performance of asphalt and found that the short-term aging performance of TLA modified asphalt could be improved significantly with an increase in the content of TLA. Heng-Long et al. [22] observed through atomic force microscope that there was a change in the interaction between asphaltene in the matrix asphalt and other components after TLA was added and that a new and more stable system was formed after modification and this significantly enhanced oxidation resistance.

The above studies have contributed to improvements in the antiaging properties of SBS-modified asphalt, but there are few studies on the composite modification of SBS-modified asphalt with nano-ZnO and TLA. Therefore, we proposed the use of nano-ZnO and TLA to modify SBS-modified asphalt. Nano-ZnO can reduce the effect of ultraviolet light on the structure of the styrene-butadiene-styrene copolymer. At the same time, TLA is used to reinforce the antioxidative aging performance of SBS-modified asphalt. Therefore, the two synergistically may improve the comprehensive antiaging ability of SBS-modified asphalt.

In order to evaluate the effect of nano-ZnO and TLA on the aging properties of SBS-modified asphalt, the physical and rheological properties of nano-ZnO/TLA/SBS composite modified asphalt after different aging modes were studied. The aging degree of composite modified asphalt under different aging modes was evaluated by residual penetration, softening point increment, complex modulus aging index, and phase angle aging index, and then the optimal mixing scheme was obtained. At the same time, the comprehensive antiaging ability of composite modified asphalt was determined by determining the colloid instability index and through infrared spectrum analysis at the micro level.

2. Experiments

2.1. Materials. In this paper, SBS-modified asphalt was selected as the base asphalt, and TLA and nano-ZnO were used as modifiers. The specific surface area of nano-ZnO was 50 m^2/g, the average particle size was 30 nm, and the purity was greater than 99.5%. Surface modification was carried out with the silane coupling agent KH-560. The performance indexes of SBS-modified asphalt and TLA are shown in Table 1.

2.2. Preparation of Composite-Modified Asphalt. In order to enable the two asphalts to be fully heated and to ensure that the SBS modifier does not fail due to excessively high processing temperatures, the SBS-modified asphalt and the TLA (20 wt%, 25 wt%, and 30 wt%) were placed in a constant temperature oven of 170°C. This was then heated to the melting state, and the asphalt was taken out from the oven and placed on an electric furnace with asbestos nets for continued heating. Then surface-modified nano-ZnO (2 wt% and 3 wt%) with a silane coupling agent (KH-570) was added and manually stirred for 2 minutes using a glass rod. Thereafter, the mixture was subjected to a high-speed shearing operation at a rotation rate of 4500 ± 400 r/min for 40 min, while maintaining the asphalt mixture at a constant temperature of 175 ± 5°C. The same operation was performed on the base asphalt to obtain a blank control sample. During the preparation of the Marshall test piece, in order to reduce the influence of the excessive viscosity of the TLA, the test piece of the asphalt mixture was extended for 10 s, so that the asphalt can better adhere to the aggregate.

Table 1: SBS-modified asphalt and TLA performance test results.

Physical properties	Unit	SBS asphalt	TLA
Penetration (25°C)	0.1 mm	53.3	2.7
Softening point	°C	76	96.5
Ductility (5°C)	cm	40.6	0.7
Viscosity (135°C)	Pa·S	2.36	75.49

2.3. Physical and Rheological Properties Test. The basic properties of the prepared asphalt samples were tested. The technical indexes included penetration at 25°C, a softening point, ductility at 5°C, and viscosity at 135°C. The corresponding tests were carried out in accordance with relevant specifications [23–26].

The rheological properties of asphalt samples were tested to study their rheological properties at medium and high temperatures. According to the test requirements of the specification [27], the complex shear modulus and phase angle were measured by a dynamic shear rheometer (DSR) in the range of 58~82°C (temperature interval, 6°C). The strain loading mode was adopted and the frequency was 10 rad/s.

2.4. Aging Procedures. The aging procedures adopted in this paper included a rotating film oven test, pressure aging test, and ultraviolet accelerated aging test, simulating short-term aging, long-term aging, and a photooxidation environment of asphalt in the field process, respectively. According to the specification for the film oven test procedure [28], the asphalt was injected into the sample dish and placed in the oven at 163°C, and the turntable rotated continuously for 5 hours at a speed of 5.5 r/min. The asphalt sample used in the pressure aging test [29] consisted of the residues of the film oven test, and the asphalt sample was placed in a pressure vessel at a test temperature of 100°C and pressure of 2.1 MPa, and the oxidation time was 20 h under pressure. A 500 W high-pressure mercury lamp as an illumination source was chosen for ultraviolet accelerated aging test. The asphalt sample after the film oven step was placed in a UV aging chamber at a temperature of 80°C for 6 days.

The physical and rheological properties of asphalt samples after the three aging tests were tested, and the degree of asphalt aging was analyzed with the residual penetration ratio (RP), softening point increment (SPI), complex modulus aging index (CMAI), and phase angle aging index (PAAI). The calculation formula of the above-mentioned indexes was as follows:

$$\begin{aligned} \mathrm{RP} &= \frac{\text{aged pentration value}}{\text{unaged pentration value}} \times 100, \\ \mathrm{SPI} &= \text{aged softening point} - \text{unaged softening point}, \\ \mathrm{CMAI} &= \frac{\text{aged complex modulus}}{\text{unaged complex modulus}} \times 100, \\ \mathrm{PAAI} &= \frac{\text{aged phase angle}}{\text{unaged phase angle}} \times 100. \end{aligned} \tag{1}$$

2.5. Analysis of Asphalt Chemical Composition. According to the specification [30], the four-component composition of the asphalt samples was tested to study the changes of the four components before and after aging of the asphalt, and the colloidal instability index of the asphalt was calculated. The formula was as follows:

$$I_c = \frac{S + A_s}{A + R}, \tag{2}$$

where S is the content of saturates in the asphalt, A is the content of the aromatics component in the asphalt, R is the content of the resins in the asphalt, and AS is the content of the asphaltenes in the asphalt.

2.6. Fourier Transform Infrared (FTIR) Characterization. Various characteristic functional groups in asphalt directly affect asphalt pavement performance. The position and shape of the infrared absorption frequency are obtained by measuring the vibration and rotation of asphalt molecules. Thus, the characteristic functional groups of asphalt can be qualitatively and quantitatively analyzed. Nexus intelligent Fourier Transform Infrared Spectrometer was used to characterize the characteristic functional groups of asphalt. The asphalt was dissolved in a sulfur dioxide (CS_2) solution, which was collocated with an asphalt-CS_2 solution with a concentration of 5%. Then the asphalt-CS_2 solution was dripped on potassium bromide (KBr) film and evaporated completely under an infrared lamp. The asphalt film was obtained and tested. The wavenumber of the film was between 4000 and 400 cm^{-1}, and the number of strokes was 120.

In order to further compare and analyze changes in the characteristic functional groups of asphalt before and after aging, the carbonyl index ($CI_{C=O}$), SBS modifier's damage index ($I_{B/S}$) [31], and sulfoxide index ($SI_{S=O}$) were used, and OMINIC infrared spectroscopy software analyzed the related areas. The formulas for calculating SBS modifier's damage index ($I_{B/S}$), carbonyl index ($CI_{C=O}$), and sulfoxide index ($SI_{S=O}$) were as follows:

$$\mathrm{CI}_{\mathrm{C=O}} = \frac{A_{1700\ \mathrm{cm}^{-1}}}{A_{(500\sim4000)\ \mathrm{cm}^{-1}}}, \tag{3}$$

$$I_{B/S} = \frac{A_{966\ \mathrm{cm}^{-1}}}{A_{699\ \mathrm{cm}^{-1}}}, \tag{4}$$

$$\mathrm{SI}_{\mathrm{S=O}} = \frac{A_{1030\ \mathrm{cm}^{-1}}}{A_{(500\sim4000)\ \mathrm{cm}^{-1}}}, \tag{5}$$

where $A_{1700\ \mathrm{cm}^{-1}}$ was the area of the carbonyl absorption peak, $A_{966\ \mathrm{cm}^{-1}}$ was the butadiene absorption peak area, $A_{699\ \mathrm{cm}^{-1}}$ was the area of the benzene ring-CH-bending vibration, and $A_{1030\ \mathrm{cm}^{-1}}$ was the area of the sulfoxide-based absorption peak. $A_{(500\sim4000)\ \mathrm{cm}^{-1}}$ was the saturated C-H absorption peak area.

3. Results and Discussion

3.1. Physical Performance Results of Different Asphalt Samples. Testing was done for three indexes of asphalt samples containing different proportion of modifiers, and the results

are shown in Table 2. With the incorporation of nano-ZnO or TLA, the penetration of SBS-modified asphalt decreases gradually, but the effect of TLA on penetration was significantly greater than that of nano-ZnO. When nano-ZnO and TLA were added to SBS asphalt at a certain proportion, the penetration still decreases considerably and is basically consistent with TLA/SBS-modified asphalt. The effect of nano-ZnO on the penetration of SBS asphalt was almost concealed by TLA. The reasons for this could be divided into two aspects: the strong surface activation energy of nano-ZnO was closely combined with asphalt and formed a state of increased stability; and TLA contained a large amount of asphaltene, where the stiffness of the asphalt system also increased along with an increase of asphaltene, and, as such, the penetration of the asphalt would decrease.

The softening point was an important indicator for the temperature sensitivity of asphalt. Table 2 shows that the incorporation of TLA or nano-ZnO had a positive effect on the improvement of softening point for SBS asphalt, for the same reasons as mentioned above. When the content of TLA was constant, the incorporation of nano-ZnO improved the softening point of composite asphalt synergistically with the former. When 3% nano-ZnO + 30% TLA was used, the softening point was 12.6°C higher than that of SBS-modified asphalt. Nano-ZnO and TLA had a better enhancement effect on the high-temperature performance of SBS asphalt.

In Table 2, nano-ZnO and TLA had different effects on the ductility of SBS asphalt. When 2%~3% nano-ZnO was added to SBS asphalt, the ductility of SBS asphalt was improved to some extent. Due to the existence of a proper amount of nano-ZnO, the expansion of the crack in the asphalt was hindered and passivated under the tensile action, and the crack eventually ended. The incorporation of TLA significantly reduced the ductility of asphalt, mainly because TLA would bring a large number of pozzolanic active mineral fine powder [32] particles, which greatly affected the binding force between the molecular structures of modified asphalt and directly led to the weakening of the low-temperature plasticity of asphalt. When TLA content exceeds 25%, ductility decreased obviously. When the amount of TLA in the asphalt exceeds 25%, the tendency of ductility decreases significantly, which indicates that the amount of TLA is not as high as possible. Rotational viscosity was characterized by viscous resistance or dynamic viscosity during the movement of the asphalt. Table 2 shows that the incorporation of nano-ZnO and TLA caused the viscosity of the SBS asphalt to increase with varying degrees. However, it was worth noting that, in the construction process of asphalt pavement, the high viscosity of asphalt would cause certain problems in the mixing, transportation, and paving compaction process of asphalt mixture. When the TLA content reaches 30%, the viscosity of the composite modified asphalt reaches 5.83 Pa·S, which results in difficulties during construction [33]. At the same time, when the TLA content is between 25% and 30%, the effect of the change in TLA content on the SBS-modified asphalt is not obvious. After comprehensive consideration, the optimal content of TLA was finally determined as 25%.

To sum up, compared with SBS asphalt, the incorporation of nano-ZnO enhanced the basic physical properties of SBS asphalt to a certain extent. In addition to weakening ductility, TLA had an obvious positive effect on other basic physical properties of SBS asphalt. Considering the influence of TLA on the ductility and rotational viscosity of composite asphalt, and to avoid the negative effect of excessive TLA on low-temperature ductility and construction of composite asphalt, the optimal content of TLA was determined as 25%, and the content of nano-ZnO needed to be further considered through additional experiments.

3.2. Dynamic Shear Rheological Properties of Different Asphalt Samples. Figure 1(a) shows that the complex modulus of the same asphalt samples decreased with an increase of temperature. This was because as the temperature increases, the flow properties of the asphalt increased, and it was easy to produce greater deformation under the same external force. Obviously, in order to produce asphalt pavement with good resistance to deformation at high temperatures, a high complex shear modulus at high temperatures was needed. Figure 1(a) shows that the incorporation of the TLA and the nano-ZnO increases the complex modulus of the composite asphalt and enhances the stiffness of the composite asphalt at the same temperature. However, when the content of TLA reached 25%, the complex modulus of the TLA/SBS composite asphalt nearly doubled compared with the average for SBS asphalt. The "hardening" effect was very obvious. When nano-ZnO was added to the TLA/SBS composite asphalt, while the complex modulus of the modified asphalt still increased, the nano-ZnO still played an active role in improving the complex modulus of asphalt with a large amount of TLA. Moreover, the complex modulus of nano-ZnO/TLA/SBS composite modified asphalt was still significantly higher than that of the other two asphalts when the temperature exceeded 80°C. This indicated that a nano-ZnO/TLA/SBS composite modified asphalt reduced permanent deformation to a certain extent under an extremely high temperature and time-temperature equivalence.

Figure 1(b) shows that, at the same temperature, with an increase of nano-ZnO content, the phase angle of nano-ZnO/SBS composite asphalt decreases. This infers that nano-ZnO slows down the conversion process of elastic components to viscous components in asphalt. When TLA was added into SBS asphalt, the phase angle of the composite modified asphalt was lower than that of SBS asphalt, and the phase angle decreases by 8°~10° at different temperatures, which indicated that TLA helps the asphalt to be more elastic. The main reason could be attributed to the fact that the TLA contained a large amount of asphaltenes, and the oil content was small. After incorporation, the rigidity of the internal structure of the asphalt increased, and the sensitivity of the asphalt molecular chain with temperature movement was lowered, which hindered the flow deformation of the asphalt molecular chain. The viscous component was reduced, so the phase angle was lowered. Both nano-ZnO and TLA can improve the deformation recovery ability of asphalt.

Table 2: Test results of basic performance of SBS asphalt under different modifier content.

Nano-ZnO content (%)	TLA content (%)	Penetration (0.1 mm)	Softening point (°C)	Ductility (cm)	Viscosity (Pa·S)
0	0	53.1	76.2	40.1	2.36
2	0	52.6	76.9	40.9	2.41
3	0	52.2	77.4	42.3	2.56
0	20	45.4	84.3	33.4	3.12
0	25	41.2	86.6	30.3	4.04
0	30	37.6	88.9	25.9	5.83
2	20	45.3	84.5	34.2	3.17
2	25	41.2	86.6	30.7	4.11
2	30	37.6	88.7	26.1	5.88
3	20	45.1	84.5	34.7	3.23
3	25	41.1	86.6	31.2	4.21
3	30	37.6	88.8	26.4	5.96

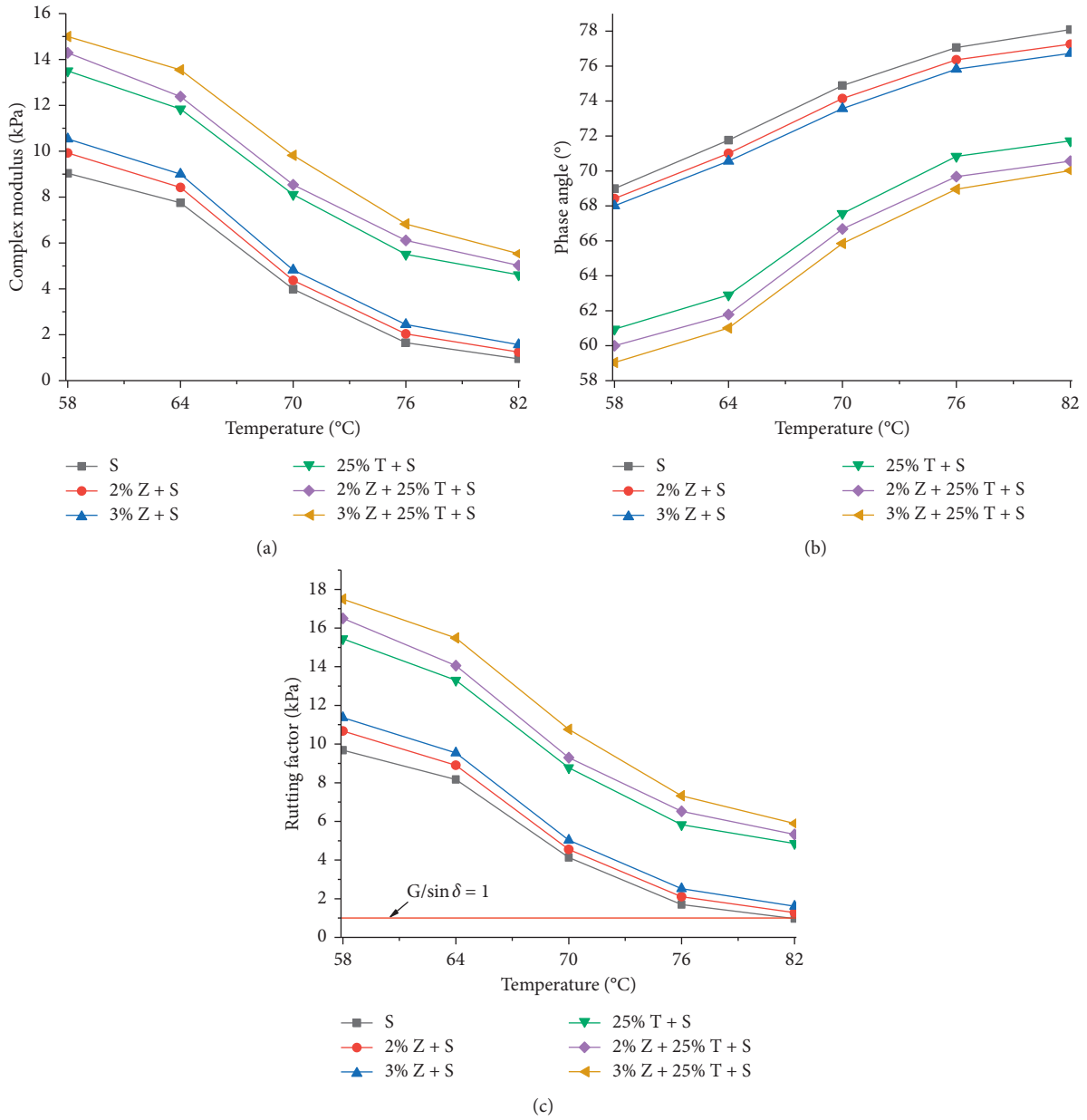

Figure 1: Effect of different content of nano-ZnO (Z) and TLA (T) on rheological properties of SBS asphalt (S). (a) Complex modulus for asphalt. (b) Phase angle for asphalt. (c) Rutting factor for asphalt.

In order to judge the performance and requirements of asphalt at different temperatures, the rutting factor ($G^*/\sin\delta$) for asphalt was used to evaluate the high-temperature rheological properties of asphalt in a SHRP plan. Table 3 shows the temperatures of several asphalts when $G^*/\sin\delta = 1$. Figure 1(c) indicates that the rutting factor of SBS asphalt gradually decreased with an increase of temperature, the flow deformation gradually becomes larger, and the rutting resistance also gradually reduced. When 2%~3% of nano-ZnO was added to SBS asphalt, the rutting factor of the nano-ZnO/SBS composite asphalt increased by 3%~11%. Because 25% of TLA brought a large amount of high-quality bitumen, the rutting factor of the TLA/SBS composite asphalt was obviously improved, and the antirutting ability became stronger. Table 3 shows that the temperature of SBS asphalt at $G^*/\sin\delta = 1$ was 81.2°C. However, when $G^*/\sin\delta = 1$ of the asphalt contained 25% of the TLA, it was more than 90°C, and, thus, TLA had an obvious effect on improving the rutting resistance of asphalt at a high temperature.

Table 3: High-temperature classification temperature of different asphalts.

Asphalt category	Temperature at $G^*/\sin\delta = 1$ kPa (°C)
SBS asphalt	81.3
2% ZnO + SBS asphalt	82.2
3% ZnO + SBS asphalt	84.3
25% TLA + SBS asphalt	>90
2% ZnO + 25% TLA + SBS asphalt	>90
3% ZnO + 25% TLA + SBS asphalt	>90

3.3. Short-Term Thermal Oxidation Aging of Different Asphalt Samples

3.3.1. Physical Properties after Short-Term Oxidation. The residual penetration (RP) ratio and softening point increment (SPI) of each group of asphalt after short-term aging are shown in Figure 2. SBS asphalt was the most seriously affected by short-term aging. The penetration of nano-ZnO/SBS asphalt was higher than that of SBS asphalt. The penetration value of SBS asphalt with 25% TLA was maintained at 86%~87%, which was about 15% higher than that of SBS asphalt. Secondly, the SBS composite modified asphalt containing TLA and nano-ZnO was the least affected. Figure 2(b) shows that the softening point of the asphalt improved after short-term aging, and the SPI of SBS asphalt reached 4.9°C, which was significantly higher than that of other asphalt groups. Adding nano-ZnO to SBS asphalt also reduced the effect of short-term thermal oxidation on SBS asphalt. This may be because the surface of nano-ZnO was tightly adsorbed by a large number of light components, which relieved the large amount of volatilization of these light components under high-temperature oxidation. At the same time, the incorporation of TLA significantly reduced the effect of aging on the softening point of asphalt, and the SPI was only half that of SBS asphalt, and the improvement effect was obvious. This was mainly because the TLA brought a large amount of colloid and asphaltene components, and its softening point generally exceeded 90°C, so the high-temperature stability of the SBS asphalt containing TLA was improved. When nano-ZnO and TLA were added to SBS asphalt at the same time, the SPI of the asphalt was still lower than that of TLA/SBS asphalt. Therefore, the two have a certain synergistic effect on improving the antiaging ability of SBS asphalt.

3.3.2. Medium-High-Temperature Shear Rheological Properties after Short-Term Oxidation. Figure 3(a) shows that the CMAI value of SBS asphalt was always higher than that of other asphalts at 58~82°C, which indicated that adding a certain amount of nano-ZnO or TLA to SBS asphalt reduced the CMAI value of asphalt. Moreover, TLA had a stronger ability to maintain its original properties after short-term aging than nano-ZnO. SBS asphalt containing 3% nano-ZnO and 25% TLA had the lowest CMAI value and was least affected by short-term aging. Figure 3(b) shows the PAAI value of each asphalt group after short-term thermal oxidation, where the PAAI value of each asphalt group tended to first decrease and then increase sharply. This was mainly due to the volatilization of light components in each asphalt group and the oxidation of colloid into asphaltene with continuous high temperature, which resulted in an increase of structural stiffness, a decrease in viscosity, and a decrease in the PAAI value of asphalt. Then, as the temperature increased to a certain value, the oxidation degradation of the SBS modifier occurred, which led to the destruction of the stable network structure of asphalt and even disintegration, such that the internal viscosity increases sharply. The fluctuation trend in Figure 3(b) shows that the incorporation of nano-ZnO or TLA into SBS asphalt reduced the impact of SBS degradation on the internal structure of asphalt. Among them, the PAAI value of nano-ZnO/TLA/SBS asphalt was relatively large, which proved that short-term thermal oxidation had a relatively small impact.

3.4. Long-Term Thermal Oxidative Aging of Different Asphalt Samples

3.4.1. Physical Properties after Long-Term Oxidation. PAV tests were carried out on asphalt residues after short-term thermal-oxidative aging. The penetration and softening point of asphalt residues were tested at 25°C. The results are shown in Figure 4. The RP of each group of asphalt showed a significant decrease. The RP value of SBS asphalt after the PAV test was only 42.54%. The RP of SBS asphalt and nano-ZnO/SBS asphalt decreased by more than 30% in short-term aging, while the RP value of SBS asphalt containing 25% TLA remained stable at about 56% after the PAV. Figure 4(b) shows the SPI values for each group of bitumen after the PAV test, where the softening point of SBS asphalt PAV was increased by 18°C, and the degree of aging was more serious. This was mainly due to the oxidation of butadiene in SBS, which generated carbonyl and sulfoxide, causing the internal network structure to disintegrate, and the light components inside the structure were released and then were oxidized and volatilized, resulting in a significant increase in the

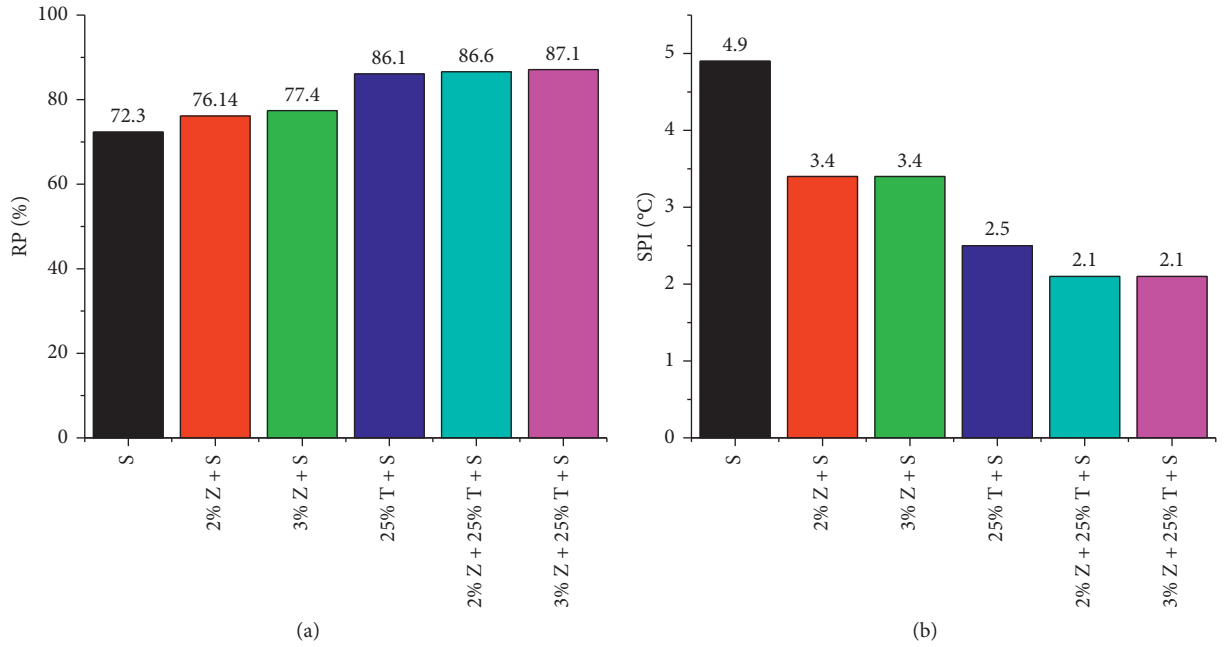

Figure 2: Effect of different content of nano-ZnO (Z) and TLA (T) on physical properties of SBS asphalt (S) after short-term aging. (a) Residual penetration for asphalt. (b) Softening point increment for asphalt.

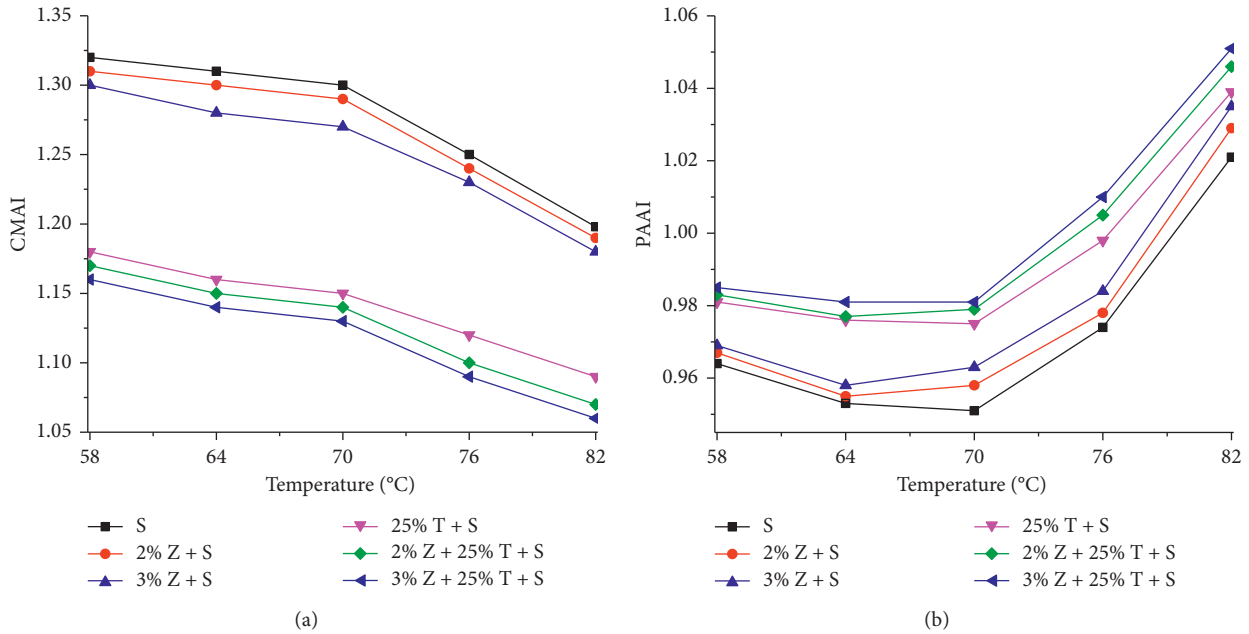

Figure 3: Effect of different amounts of nano-ZnO (Z) and TLA (T) on rheological properties of SBS asphalt (S) after short-term aging. (a) Complex modulus aging index for asphalt. (b) Phase angle aging index for asphalt.

softening point of SBS asphalt. The increase in SBS asphalt containing nano-ZnO was comparable to that of SBS asphalt, and nano-ZnO provided no significant improvement in the long-term thermal oxidative aging properties of SBS asphalt. However, the increase in the softening point of the TLA/SBS asphalt after PAV was obviously less than that of SBS asphalt, which was only half of the latter, and the improvement effect was very obvious. The reason was basically consistent with short-term aging. Therefore, the above results indicated that SBS asphalt containing TLA had better resistance to long-term aging.

3.4.2. Medium-High-Temperature Shear Rheological Properties after Long-Term Oxidation. The CMAI values of SBS asphalt and nano-ZnO/SBS asphalt were stable in the range of 3.0–3.6 and SBS asphalt containing TLA was stable in the range of 1.5–2.5, as shown in Figure 5. TLA greatly reduced

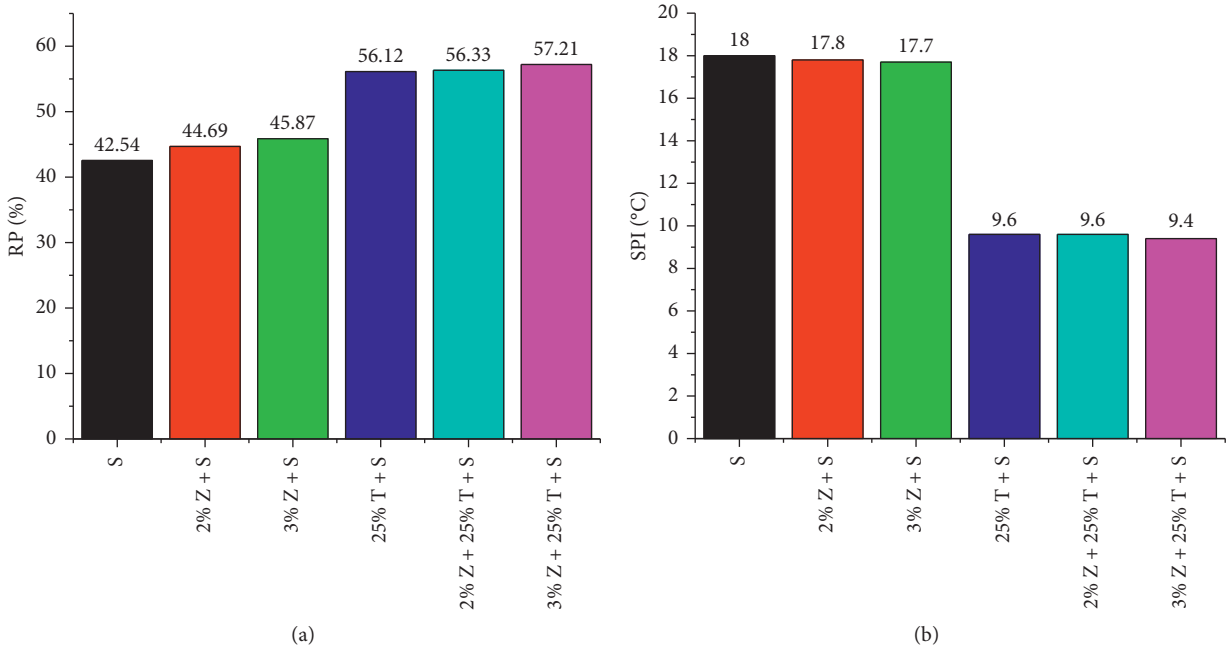

Figure 4: Effect of different content of nano-ZnO (Z) and TLA (T) on physical properties of SBS asphalt (S) after long-term aging. (a) Residual penetration for asphalt. (b) Softening point increment for asphalt.

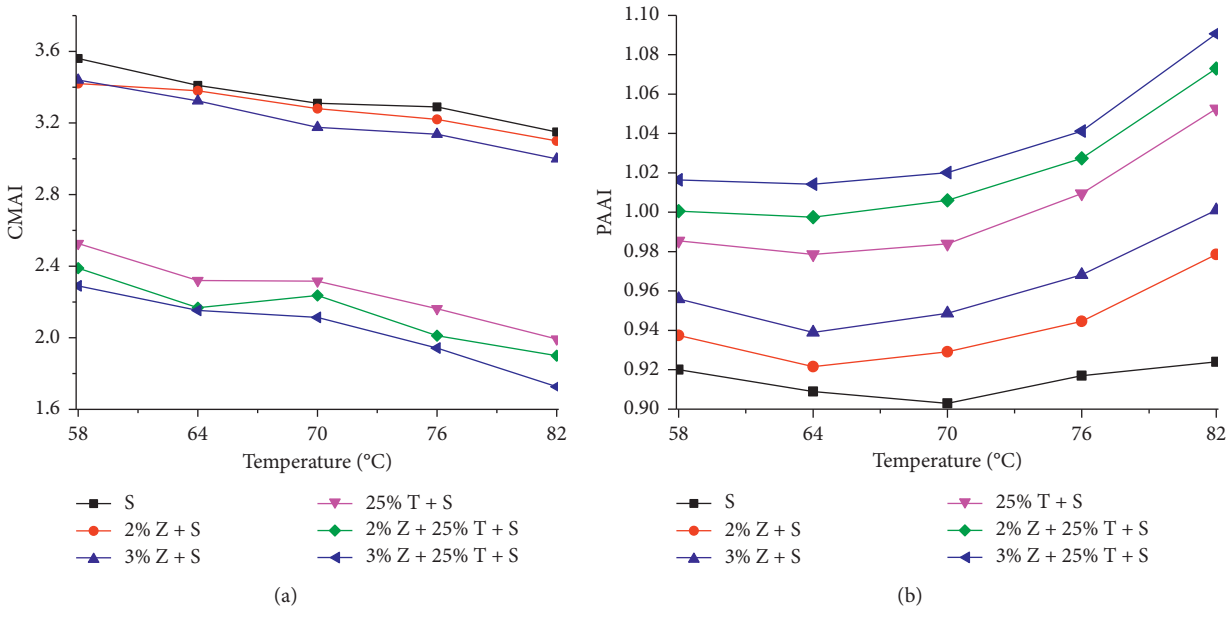

Figure 5: Effect of different content of nano-ZnO (Z) and TLA (T) on rheological properties of SBS asphalt (S) after long-term aging. (a) Complex modulus aging index for asphalt. (b) Phase angle aging index for asphalt.

the CMAI of composite asphalt, mainly because TLA brought a large number of high-quality asphaltenes. Such asphaltenes have existed for thousands of years and thus the physical properties were relatively stable, and its reaction with oxygen was relatively slow, thus reducing the CMAI of asphalt. According to Figure 5(b), the PAAI of SBS asphalt increased with the addition of nano-ZnO and TLA, and the growth of nano-ZnO/TLA/SBS asphalt was the most obvious. Accordingly, this infers that there was an effect of pressurized oxidation on asphalt: SBS asphalt > nano-ZnO/SBS asphalt > nano-ZnO/TLA/SBS asphalt.

3.5. UV Oxidation Aging of Different Asphalt Samples

3.5.1. Physical Properties after UV Oxidation. The UV aging test of asphalt residues after short-term thermal oxidation aging was carried out to simulate a real photooxidation process. Figure 6 shows that, after adding 2% nano-ZnO to SBS-modified asphalt, there was no obvious difference in RP, but the

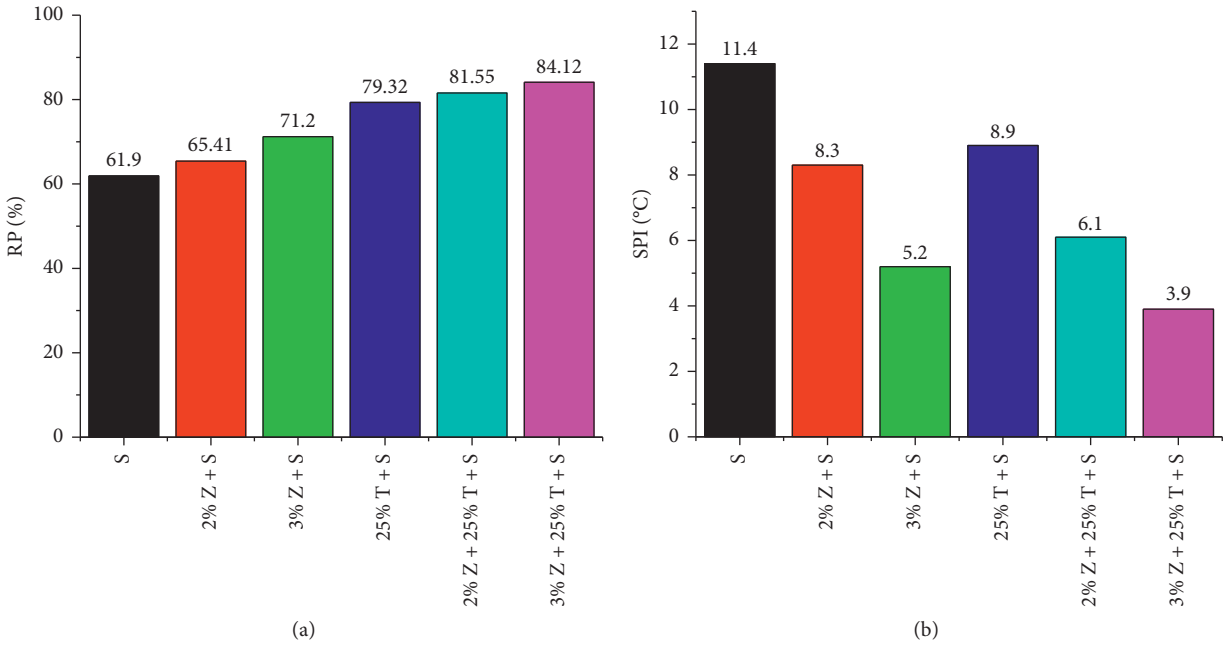

Figure 6: Effect of different content of nano-ZnO (Z) and TLA (T) on physical properties of SBS asphalt (S) after UV aging. (a) Residual penetration for asphalt. (b) Softening point increment for asphalt.

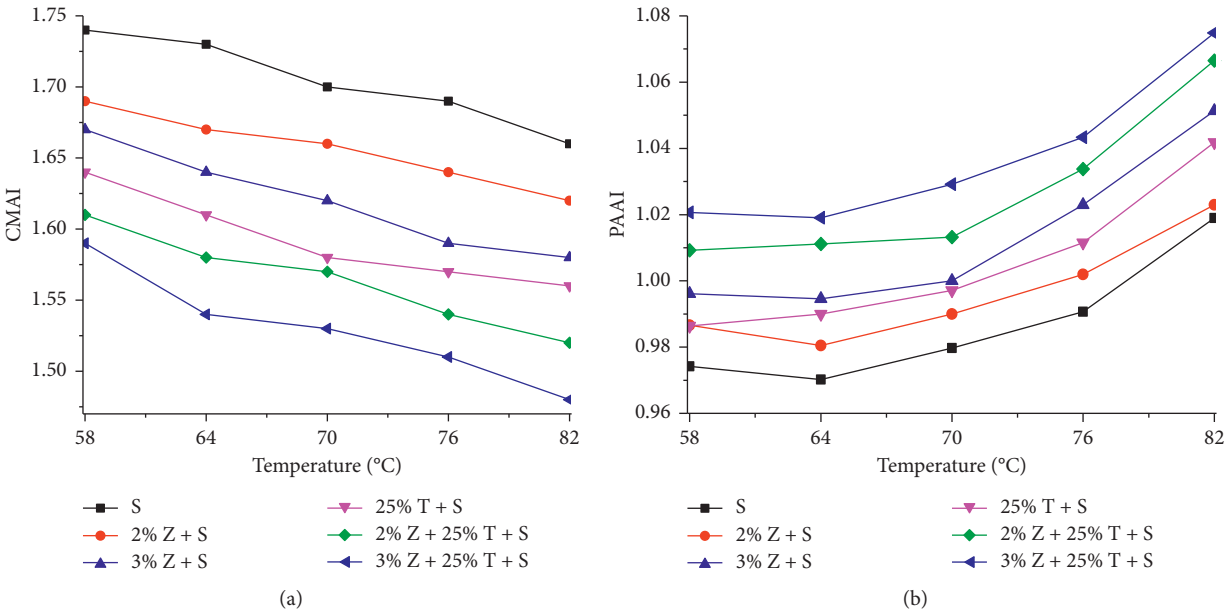

Figure 7: Effect of different content of nano-ZnO (Z) and TLA (T) on rheological properties of SBS asphalt (S) after short-term aging. (a) Complex modulus aging index for asphalt. (b) Phase angle aging index for asphalt.

penetration ratio of SBS asphalt containing TLA increased significantly compared with SBS-modified asphalt. Figure 6(b) shows that SBS had the largest SPI value, and the other groups of asphalt had a certain degree of decline. The SPI values of TLA/SBS asphalt and nano-ZnO/TLA/SBS asphalt changed with the increase in content of nano-ZnO, and the latter showed a maximum decrease of nearly 56% on the basis of the former. This was mainly due to the fact that nano-ZnO absorbed and provided shielding from ultraviolet rays, thereby reducing the influence of ultraviolet rays on the performance degradation of SBS asphalt, and improved asphalt resistance to ultraviolet aging.

3.5.2. Medium-High-Temperature Shear Rheological Properties after UV Oxidation. The CMAI and PAAI of each group of asphalt after UV aging are shown in Figure 7. In the test temperature range, the incorporation of nano-ZnO and TLA

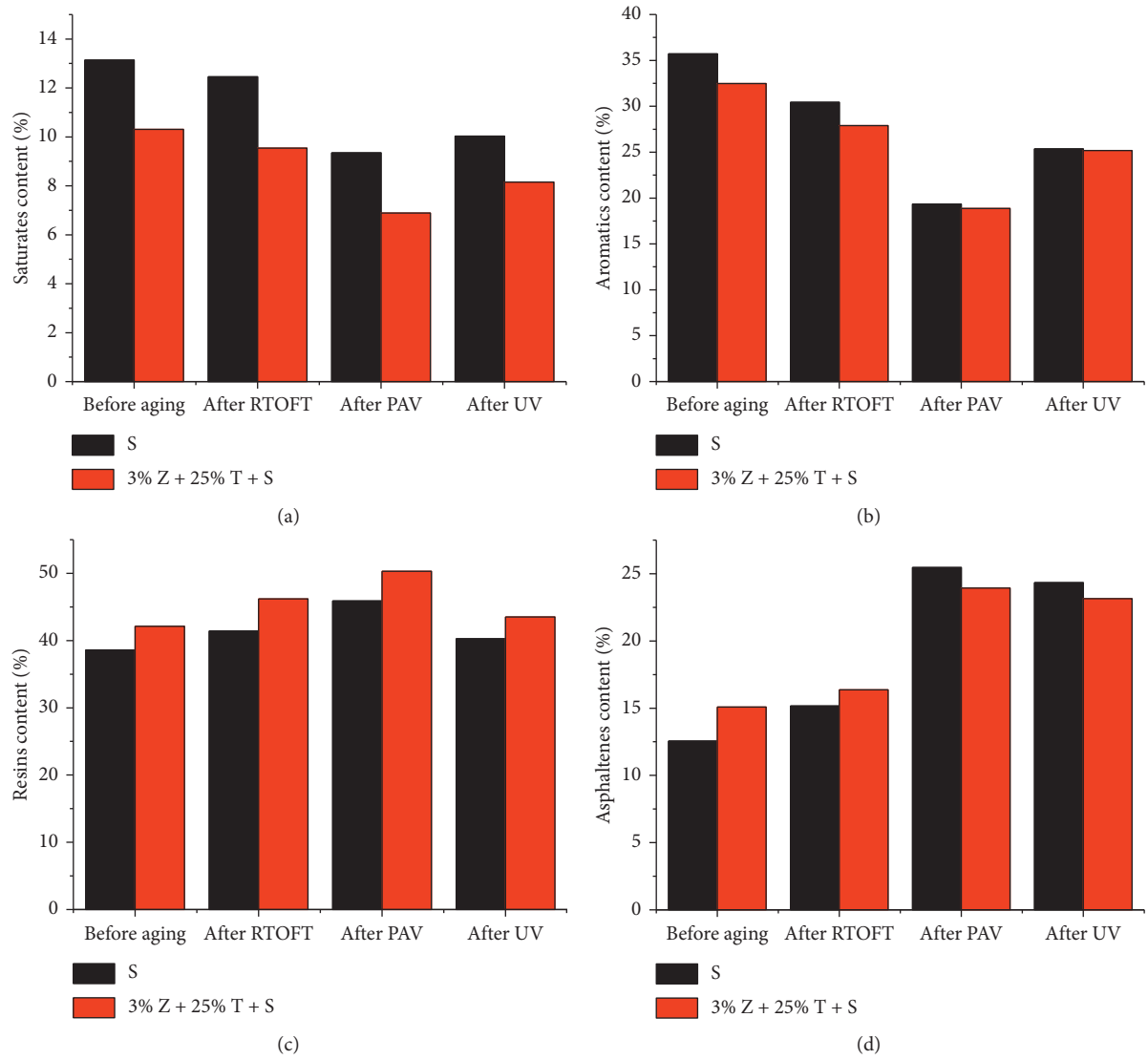

Figure 8: Effect of nano-ZnO (Z) and TLA (T) on the composition of SBS asphalt (S) after aging. (a) Saturates content for asphalt. (b) Aromatics content for asphalt. (c) Resins content for asphalt. (d) Asphaltenes content for asphalt.

reduced the CMAI value of SBS asphalt and increased the PAAI value, and the effect was obvious after adding nano-ZnO. Notably, the CMAI value and PAAI value of the TLA/SBS asphalt were between 2% and 3% nano-ZnO/SBS asphalt, which may be due to the role of ash in the TLA. The PAAI of SBS-modified asphalt with 2% Z + 25% T and SBS-modified asphalt with 3% Z + 25% T was greater than 1, which shows that nano-ZnO and TLA can reduce the influence of ultraviolet on the rheological properties of asphalt, and both of them can maintain their original state. However, due to the splitting of a small amount of SBS modifier under UV light, the elastic component was released, which eventually leads to the increase of asphalt phase angle. At the same time, 3% nano-ZnO + 25% TLA SBS composite asphalt had the smallest CMAI value and the largest PAAI value, indicating better reduction of the degradation effect of ultraviolet light on the rheological properties of SBS asphalt. Therefore, considering the changes in basic physical properties and rheological properties of SBS asphalt before and after aging, the final recommended proportion from this study was a SBS composite asphalt of 3% nano-ZnO + 25% TLA.

3.6. Analysis of Components after Aging of Different Asphalt Samples. In order to analyze the influence of asphalt composition and the colloidal instability index on performance under different aging conditions, the components of SBS asphalt and recommended proportions before and after aging were analyzed. The changes in asphalt composition before and after aging are shown in Figure 8. After incorporation of TLA into SBS asphalt, the mass fraction of saturated and aromatic components in composite asphalt decreased and the content of resin and asphaltene increased, which proved that TLA brought abundant recombinant components to SBS asphalt. Comparing the changes of components in asphalt before and after aging, the content of saturated and aromatic components in asphalt gradually decreased, while the content of resin and asphaltene

gradually increased. This indicated that the light components volatilize in different degrees during aging, and dehydrogenation and condensation of asphalt occurred in a hot or photo-oxygen-rich environment. The molecular weight of the asphalt increased gradually, and the light components gradually changed to the recombinant components. From the growth rate of colloid and asphaltene, the growth rate of heavy components in SBS asphalt containing TLA and nano-ZnO during aging was significantly lower than that of SBS asphalt. This indicated that the incorporation of TLA and nano-ZnO inhibited the conversion of light components into heavy components in SBS asphalt to a certain extent and reduced the effect of aging on SBS asphalt.

Siddiqui [34] believed that the Gastel index (I_c) provides a good reflection of the peptization ability of asphalt, and it could also reflect the change of colloid performance after the asphalt aging process. The smaller I_c is, the better the peptizing ability of the asphalt is, and the more it tended to be a melt-gel type structure, where the asphalt was more stable, and the pavement performance was better. The colloidal instability index (I_c) of each group of pitch was calculated according to a formula (2), and the results are shown in Table 4. Table 4 shows that the I_c values of the two asphalts before aging were similar, and after a period of short-term aging, I_c of the SBS asphalt increased by 8.5%. The growth rate of nano-ZnO/TLA/SBS asphalt was only 2.9%, which showed that the short-term aging had little effect on the latter. After long-term aging, the colloidal instability index of the two kinds of asphalt increased sharply. I_c of SBS asphalt reached 0.53, and the growth rate reached 51.4%, while the growth of I_c of nano-ZnO/TLA/SBS asphalt was only 32.4%. After UV aging, the I_c value of SBS asphalt increased by 48.6%, and I_c of nano-ZnO/TLA/SBS asphalt increased by 35.3%. The above results showed that the incorporation of nano-ZnO and TLA greatly reduced the growth rate of I_c after the aging of SBS asphalt, reducing the effect of aging on SBS asphalt, delaying the conversion of SBS asphalt to gel asphalt, and enhancing the aging resistance of SBS asphalt.

3.7. Analysis of Characteristic Functional Groups in Asphalt

3.7.1. Infrared Spectroscopy Analysis of Asphalt before Aging. The characteristic functional groups of SBS asphalt, TLA, and 3% ZnO + 25% TLA + SBS asphalt were scanned. The infrared spectra of the three asphalts are shown in Figure 9. The results of the corresponding functional groups are shown in Table 5. Figure 9 shows that the TLA asphalt exhibited a strong absorption peak at 3458 cm^{-1}, which was caused by the stretching vibration of O-H at the surface of the TLA. At the same time, there were obvious absorption peaks of TLA at 1030 cm^{-1}. It was noteworthy that there were overlapping peaks between the antisymmetric absorption peaks of silicon Si-O-Si functional groups formed by ash (mainly quartz and clay) and the stretching vibration peaks of sulfoxide group S=O functional groups in TLA. This led to the inaccurate measurement of sulfoxide content in asphalt, and, as such, the calculation for sulfoxide index (SI) in a later period was cancelled. Unlike SBS asphalt, the other two asphalts had strong absorption peaks at 440 cm^{-1}, which was due to the overlap of the absorption peaks of Zn-O and silicon Si-O-Si.

Table 4: Calculation results of asphalt colloid instability index.

Aging state	SBS asphalt		3% Z + 25% T + SBS asphalt	
	I_c	I_c increment	I_c	I_c increment
Before aging	0.346	—	0.340	—
RTFOT	0.385	0.039	0.350	0.009
PAV	0.534	0.188	0.446	0.096
UV	0.524	0.178	0.456	0.115

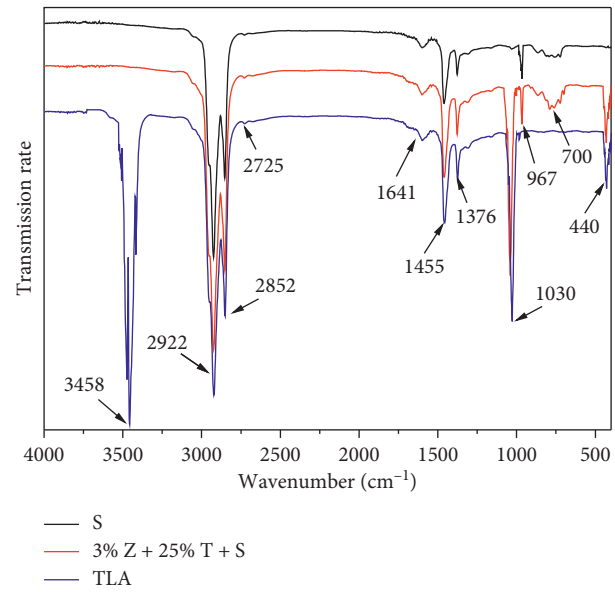

Figure 9: Effect of nano-ZnO (Z) and TLA (T) on infrared spectrum of SBS asphalt (S).

3.7.2. Infrared Spectroscopy Analysis of Asphalt after Aging. The infrared spectrum of the asphalt was scanned, and the scanning results are shown in Figure 10. OMINIC infrared spectroscopy software was used to calculate the relevant area before and after aging by formulas (3)~(4). The carbonyl index ($CI_{C=O}$) and SBS modifier's damage index ($I_{B/S}$) of the two kinds of asphalt were quantitatively calculated. The calculation results are shown in Table 6. As the aging process intensified, the change in the carbonyl index of SBS asphalt increased from 0.143 to 0.371, indicating that the carbon chain in SBS asphalt was gradually oxidized to form carbonyl. $I_{B/S}$ decreased slowly with short-term aging but decreased sharply under ultraviolet aging and long-term aging conditions, indicating that the performance of SBS asphalt was mainly affected by ultraviolet aging and long-term aging. In addition, the changes in the carbonyl index of 3% ZnO + 25% TLA + SBS asphalt were in the range of 0.116~0.213, and the decrease in $I_{B/S}$ was in the range of 0.021~0.199, which was obviously smaller than that of SBS asphalt. The above test results proved that the incorporation of TLA and nano-ZnO effectively inhibited the formation of

Table 5: Asphalt functional group results.

Absorption wavenumber (cm^{-1})	Corresponding functional group	SBS asphalt	TLA	3% Z + 25% T + SBS asphalt
3458	O-H stretching vibration	×	✓	×
2922	-CH_2-asymmetric stretching vibration	✓	✓	✓
2852	-CH_2-symmetric stretching vibration	✓	✓	✓
2725	-CHO stretching vibration	✓	✓	✓
1743	Carbonyl C=O stretching vibration	✓	✓	✓
1455	-CH_2-bending vibration	✓	✓	✓
1376	-CH_3-umbrella vibration	✓	✓	✓
1030	Sulfoxide-based S=O stretching vibration	✓	✓	✓
1030	Si-O-Si stretching vibration	×	✓	✓
967	Butadiene C=C stretching vibration	✓	×	✓
700	Benzene ring-CH-bending vibration	✓	×	✓
440	Si-O-Si stretching vibration	×	✓	✓

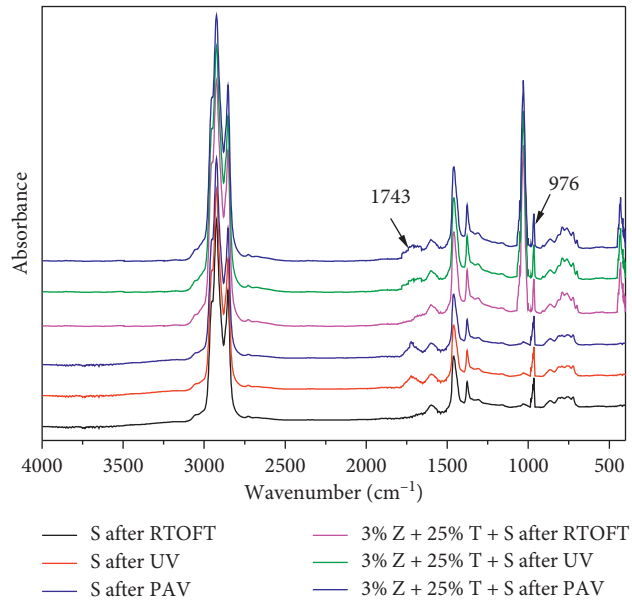

Figure 10: Effect of nano-ZnO (Z) and TLA (T) on aging of SBS asphalt (S).

a carbonyl group and breakage of the C=C double bond in butadiene and further verified that the incorporation of TLA and nano-ZnO enhanced the comprehensive antiaging ability of SBS asphalt.

3.8. Summary of Experimental Results. The rheology (76°C), SARA, and FTIR results of SBS-modified asphalt and 3% ZnO + 25% TLA + SBS asphalt are summarized, as shown in Table 7. After RTFOT aging, the light components in the SBS-modified asphalt are volatilized, and the asphaltene content increases, resulting in increased internal stiffness in the asphalt. The complex shear modulus of SBS asphalt increases, the phase angle decreases, and eventually the performance of the asphalt decreases. 3% ZnO + 25% TLA + SBS asphalt has a small change in various performance indicators after RTFOT aging and is less affected by aging. After PAV aging, the change of various performance indicators of 3% ZnO + 25% TLA + SBS asphalt is also much smaller than that of SBS-modified asphalt. SBS-modified asphalt increased by nearly 54% for I_C. The 3% ZnO + 25% TLA + SBS asphalt was only 31%, which indicates that the internal composition of SBS-modified asphalt changed drastically after PAV aging. After UV aging, the carbonyl content in SBS-modified asphalt increased significantly, and $I_{B/S}$ decreased by nearly 0.288.3% ZnO + 25%. TLA + SBS asphalt has an increase in carbonyl content of only 0.169, and the residual SBS-modifier content is also much larger than that of SBS-modified asphalt. This shows that the addition of 3% nano-ZnO and 25% TLA significantly improves the comprehensive antiaging ability of SBS-modified asphalt.

During the thermal oxygen aging process, the carbon chain is constantly broken and reacts with the oxygen element to form a carbonyl group. Associative reactions between these polarities continue to occur, thereby destroying the original stable structure of the asphalt colloid, the asphalt becomes hard, and the performance of the asphalt continues to deteriorate. The addition of TLA injected a large amount of light components into the asphalt, which itself is the oxidation product of nature for millions of years. The

Table 6: Table of changes in asphalt carbonyl index (CI) and styrene index ($I_{B/S}$) before and after aging.

Aging state	SBS asphalt				3% Z + 25% T + SBS asphalt			
	CI	CI increment	$I_{B/S}$	$I_{B/S}$ reduction	CI	CI increment	$I_{B/S}$	$I_{B/S}$ reduction
Before aging	0.114	—	1.882	—	0.154	—	1.873	—
RTFOT	0.257	0.143	1.835	0.047	0.27	0.116	1.852	0.021
UV	0.337	0.223	1.594	0.288	0.323	0.169	1.674	0.199
PAV	0.485	0.371	1.644	0.238	0.367	0.213	1.715	0.158

Note. Z was ZnO; T was TLA.

Table 7: Summary of experimental results.

Aging state	SBS asphalt					3% Z + 25% T + SBS asphalt				
	CMAI	PAAI	I_C	CI	$I_{B/S}$	CMAI	PAAI	I_C	CI	$I_{B/S}$
Before aging	—	—	0.346	0.114	1.882	—	—	0.34	0.154	1.873
RTFOT	1.25	0.974	0.385	0.257	1.835	1.09	1.01	0.35	0.27	1.852
PAV	3.29	0.917	0.534	0.485	1.644	1.94	1.04	0.446	0.367	1.715
UV	1.69	0.991	0.524	0.337	1.594	1.51	1.05	0.456	0.323	1.674

chemical structure of TLA is very stable, which greatly reduces the effect of thermal oxygen aging on asphalt. During the UV aging process, the active groups in the asphalt and styrene-butadiene-styrene copolymer are constantly broken under the irradiation of ultraviolet rays. Some groups generate carbonyl groups. The C=C double bond in the styrene-butadiene-styrene copolymer is broken by energy absorption and eventually degrades, resulting in the failure of the SBS modifier. The existence of Nano-ZnO greatly absorbs and shields from ultraviolet radiation, reducing the impact of ultraviolet aging on asphalt, and delays the degradation of asphalt performance. Asphalt pavement is continuously affected by thermal oxygen aging and ultraviolet aging in the actual use process. Due to the simultaneous existence of nano-ZnO and TLA, the two will always reduce the aging and affect the asphalt, thus synergistically improving the comprehensive antiaging ability of the asphalt.

4. Conclusion

In order to improve the antiaging ability of SBS-modified asphalt, the effects of nano-ZnO and TLA on the physical properties, rheological properties, four components, and characteristic functional groups of SBS asphalt before and after aging were studied in this paper. The main research conclusions were as follows:

(1) After adding nano-ZnO and TLA to SBS-modified asphalt, the physical and rheological properties of SBS-modified asphalt were improved to varying degrees. In particular, the addition of lake asphalt can significantly improve the high-temperature performance of SBS-modified asphalt.

(2) Combining the changes of physical properties and rheological properties before and after RTOFT, PAV, and UV aging, the recommended proportion ratio was confirmed as 3% nano-ZnO + 25% TLA.

(3) Under three aging modes, the growth rate of heavy components in SBS asphalt was significantly higher than the recommended solution. At the same time, the growth rate of the colloidal instability index (I_C) of the recommended scheme was also lower than that of SBS asphalt.

(4) Infrared spectral scanning results show that the proposed scheme can effectively inhibit the rapid increase of carbonyl content in SBS-modified asphalt and the rupture of the C=C double bond in butadiene. The recommended scheme significantly reduced the degradation effect of ultraviolet aging and long-term aging on the performance of SBS asphalt and synergistically improved the comprehensive antiaging ability of SBS-modified asphalt.

Data Availability

The data used to support the findings of this study are included within the article.

Conflicts of Interest

The authors declare that they have no conflicts of interest.

Acknowledgments

The authors would like to acknowledge the financial support of the National Natural Science Foundation of China (Grant no. 51978083) and the financial support of China Scholarship Council (Grant no. 201808430101).

References

[1] M. Liang, P. Liang, W. Fan, C. Qian, X. Xin, and G. Nan, "Thermo-rheological behavior and compatibility of modified asphalt with various styrene-butadiene structures in SBS copolymers," *Materials & Design*, vol. 88, pp. 177–185, 2015.

[2] Y. Ruan, R. R. Davison, and C. J. Glover, "Oxidation and viscosity hardening of polymer-modified asphalts," *Energy & Fuels*, vol. 17, no. 4, pp. 991–998, 2003.

[3] M. S. Cortizo, D. O. Larsen, H. Bianchetto, and J. L. Alessandrini, "Effect of the thermal degradation of SBS copolymers during

the ageing of modified asphalts," *Polymer Degradation and Stability*, vol. 86, no. 2, pp. 275–282, 2004.

[4] S.-P. Bianchetto, L. Pang, L.-T. Mo, Y.-C. Chen, and G.-J. Zhu, "Influence of aging on the evolution of structure, morphology and rheology of base and SBS modified bitumen," *Construction and Building Materials*, vol. 23, no. 2, pp. 1005–1010, 2009.

[5] H.-L. Zhang, M.-M. Su, S.-F. Zhao, Y.-P. Zhang, and Z.-P. Zhang, "High and low temperature properties of nano-particles/polymer modified asphalt," *Construction and Building Materials*, vol. 114, pp. 323–332, 2016.

[6] S. S. Sun, Y. M. Wang, and A. Q. Zhang, "Study on anti-ultraviolet radiation aging property of TiO_2 modified asphalt," *Advanced Materials Research*, vol. 306-307, pp. 951–955, 2011.

[7] M. Saltan, S. Terzi, and S. Karahancer, "Performance analysis of nano modified bitumen and hot mix asphalt," *Construction and Building Materials*, vol. 173, pp. 228–237, 2018.

[8] L. Sun, X. Xin, and J. Ren, "Asphalt modification using nano-materials and polymers composite considering high and low temperature performance," *Construction and Building Materials*, vol. 133, pp. 358–366, 2017.

[9] H. Y. Liu, H. L. Zhang, P. W. Hao, and C. Z. Zhu, "The effect of surface modifiers on ultraviolet aging properties of nano-zinc oxide modified bitumen," *Petroleum Science and Technology*, vol. 33, no. 1, pp. 72–78, 2015.

[10] H. Yao, Q. Dai, and Z. You, "Fourier transform infrared spectroscopy characterization of aging-related properties of original and nano-modified asphalt binders," *Construction and Building Materials*, vol. 101, pp. 1078–1087, 2015.

[11] H. Yao, Z. You, and L. Li, et al., "Rheological properties and chemical bonding of asphalt modified with nanosilica," *Journal of Materials in Civil Engineering*, vol. 25, no. 11, pp. 1619–1630, 2013.

[12] P. F. Du, N. X. Ke, and H. L. Zhang, "Effect of nano-zinc oxide on the morphology and ultraviolet aging properties of various bitumen," *Petroleum Science and Technology*, vol. 33, no. 10, pp. 1110–1117, 2015.

[13] M. Arabani, A. K. Haghi, and V. Shakeri, "Experimental modeling the creep compliance behavior of modified asphalt mixtures with nano-zinc oxide," *Journal of Polymer Research*, vol. 8, no. 3, p. 131, 2014.

[14] P. Xiao and X. F. Li, "Research on the performance and mechanism of nanometer ZnO/SBS modified asphalt," *Journal of Highway and Transportation Research and Development*, vol. 24, pp. 12–16, 2007, in Chinese.

[15] Y. Z. Chen, A. J. Chen, C.-J. Li, and Z.-X. Li, "Analysis of Performance for Nano-ZnO modified asphalt mixture," *China Journal of Highway and Transport*, vol. 7, pp. 25–32, 2017, in Chinese.

[16] P. Sun, H. L. Zhang, G. Guo, and D. Niu, "Pavement performance of Nano-composite modified asphalt mixture," *Journal of Building Materials*, vol. 4, pp. 672–677, 2016, in Chinese.

[17] M. M. Su, H. L. Zhang, J. Lv, and Y. Zhang, "Experimental study on high temperature performance of nano-composite modified asphalt and its mixture at extreme high temperature," *Journal of Chongqing Jiaotong University*, vol. 37, no. 3, pp. 27–33, 2018, in Chinese.

[18] R. Li, F. Xiao, S. Amirkhanian, Z. You, and J. Huang, "Developments of nano materials and technologies on asphalt materials–a review," *Construction and Building Materials*, vol. 143, pp. 633–648, 2017.

[19] C. Fang, R. Yu, S. Liu, and Y. Li, "Nanomaterials applied in asphalt modification: a review," *Journal of Materials Science & Technology*, vol. 29, no. 7, pp. 589–594, 2013.

[20] R. Li, P. Wang, B. Xue, and J. Pei, "Experimental study on aging properties and modification mechanism of Trinidad lake asphalt modified bitumen," *Construction and Building Materials*, vol. 101, pp. 878–883, 2015.

[21] J. Liu, K. Yan, J. Liu, and D. Guo, "Evaluation of the characteristics of Trinidad Lake asphalt and styrene-butadiene-rubber compound modified binder," *Construction and Building Materials*, vol. 202, pp. 614–621, 2019.

[22] Z. Heng-Long, Y. U. Jian-Ying, L. I. Qi-Gang, L. Qi-Gang, and L. Rong, *A Study on Properties and Mechanism of TLA Modified Asphalt*, Highway, Beijing, China, 2010, in Chinese.

[23] ASTM D5, *Standard Test Method for Penetration of Bituminous Materials*, ASTM, West Conshohocken, PA, USA, 2013.

[24] ASTM D36, *Standard Test Method for Softening Point of Bitumen (Ring-And-Ball Apparatus)*, ASTM, West Conshohocken, PA, USA, 2012.

[25] ASTM D113, *Standard Test Method for Ductility of Bituminous Materials*, ASTM, West Conshohocken, PA, USA, 2007.

[26] ASTM D4402, *Standard Test Method for Viscosity Determination of Asphalt at Elevated Temperatures Using a Rotational Viscometer*, ASTM, West Conshohocken, PA, USA, 2012.

[27] ASTM D7175, *Standard Test Method for Determining the Rheological Properties of Asphalt Binder Using a Dynamic Shear Rheometer (DSR)*, ASTM, West Conshohocken, PA, USA, 2015.

[28] ASTM D2872, *Standard Test Method for Effect of Heat and Air on a Moving Film of Asphalt (Rolling Thin-Film Oven Test)*, ASTM, West Conshohocken, PA, USA, 2012.

[29] ASTM D6521, *Standard Practice for Accelerated Aging of Asphalt Binder Using a Pressurized Aging Vessel (PAV)*, ASTM, West Conshohocken, PA, USA, 2013.

[30] ASTM D4124, *Standard Test Method for Separation of Asphalt into Four Fractions*, ASTM, West Conshohocken, PA, USA, 2018.

[31] C. Yan, W. Huang, F. Xiao, L. Wang, and Y. Li, "Proposing a new infrared index quantifying the aging extent of SBS-modified asphalt," *Road Materials and Pavement Design*, vol. 19, no. 6, pp. 1406–1421, 2018.

[32] R. He, S. Zheng, H. Chen, and D. Kuang, "Investigation of the physical and rheological properties of Trinidad lake asphalt modified bitumen," *Construction and Building Materials*, vol. 203, pp. 734–739, 2019.

[33] JTG E20-2011, *The Chinese Standard Test Methods of Bitumen and Bituminous Mixtures for Highway Engineering*, Renmin Communication Press, Beijing, China, 2011, http://www.doc88.com/p-4611318671004.html.

[34] M. Heitzman, *Design and Construction of Asphalt Paving Materials with Crumb Rubber Modifier*, Transportation Research Record, Federal Highway Administration, Washington, DC, USA, 1999.